

ASTRO Final Report: Identification of Carbon Cycle Extremes Using Earth System Models

Bharat Sharma

30th May 2017 – 22nd December 2017

Abstract

This study analyzes how climate extremes like droughts and heatwaves affect terrestrial carbon cycles from 1850 to 2300, using CESM1-BGC model data. It finds that thresholds for extreme events rise over time, making today's extremes less exceptional in the future. Both positive and negative extremes are increasing, but carbon loss from negative events is growing faster than gains from positive events, threatening the future stability of the land carbon sink and likely leading to higher atmospheric CO₂ if trends persist. The intensity and spatial extent of negative extremes are projected to increase globally, especially after 2100. Analysis also shows precipitation-evapotranspiration anomalies are the dominant climate driver behind these extremes, with the most significant impacts occurring without a time lag. In the South American tropics, regional trends are tied to climate-driven changes in vegetation, such as dieback due to hotter, drier conditions

1 Introduction

Terrestrial ecosystems are affected by climate extremes such as droughts and heatwaves which have a potential to modify carbon budgets. Previous studies have found the impact of negative extremes in gross primary production (GPP) and net ecosystem production (NEP) to be diminishing towards the end of the 21st century relative to the overall increase in global carbon uptake. A few studies have estimated that the land use changes (e.g. from forest to croplands) would cause more cumulative carbon loss between 1850 and 2300 than due to climate change caused by anthropogenic forcing over the same interval. However, not many studies have looked at the impact of carbon cycle extremes beyond 21st century.

The project that I did here had following parts:

1. Definition of extreme events in carbon cycle
2. Identification of extreme events globally as well as for plant functional types
3. Using image-processing tool to find spatio-temporal contiguous extreme events
4. Finding the correlation of the carbon-cycle extreme events with climate drivers
5. Attribution of extreme events to climate drivers using Multi-Linear Regression

As an example, figure 1 shows the spatial distribution of the frequency of negative extreme events for the time period 2175–2199 and the threshold for defining the extreme events is 1.0 percentile.

The data source for this study is Community Earth Science Model named CESM1-BGC. The model consists of historical (1850–2005), representative concentration pathway 8.5 (2006–2100) and extended concentration pathway 8.5 (2101–2300). It is a monthly mean data, the resolution is 0.9375° × 1.25° (latitude × longitude) and the land-use is constant based on the pre-industrial forcing.

The main reason to use the model output after 2100 and until 2300 is because the positive feedback becomes large after 2100.

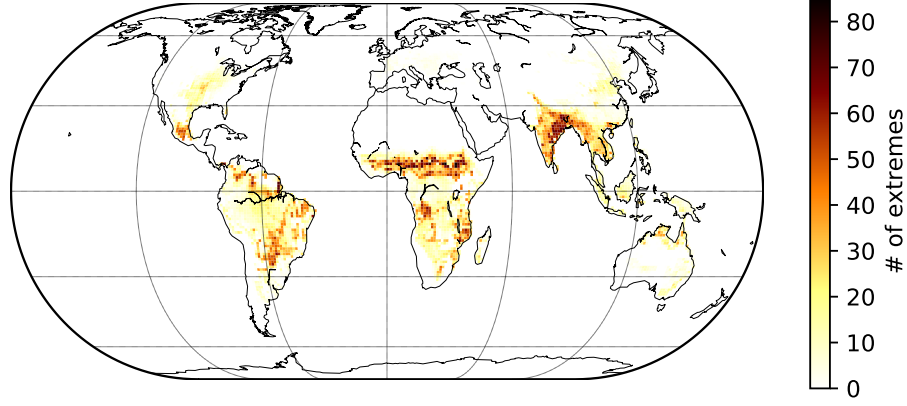


Figure 1: Frequency of negative extreme events for 2175–2199, percentile: 1.0

2 Results and Conclusions

According to the CESM1-BGC, the results (based on 25–year consecutive window and 1.0 percentile) and conclusions of this study are:

1. The figure 2 shows the increasing thresholds with time for an event to be considered extreme. It can be noticed that a current positive or negative extreme event, would not be considered an extreme event after five decades.

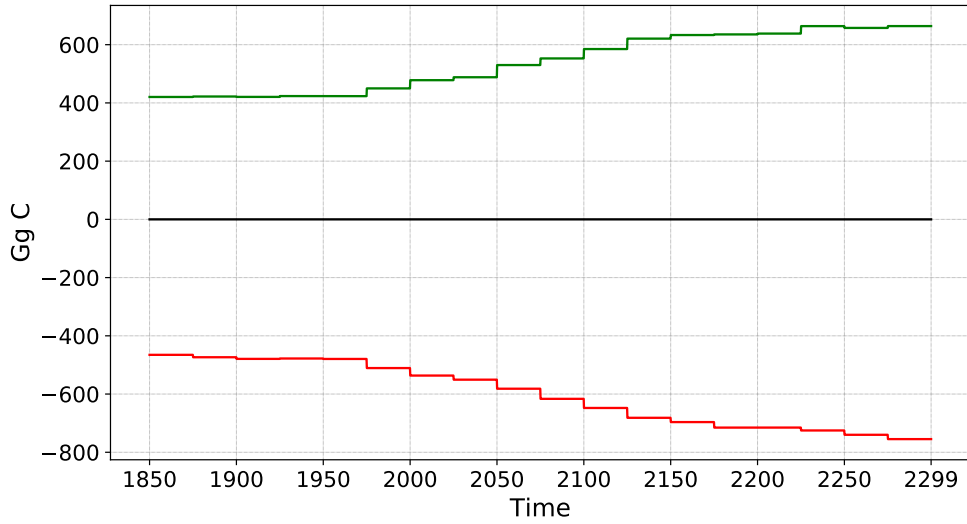


Figure 2: Thresholds when percentile is 1.0 and time period is 25 years

2. The figure 3 shows the increasing frequency of positive as well as negative extreme events based on the threshold of the time period 1850–1999. The rate of increase of the negative extreme events is higher than the positive extreme events.

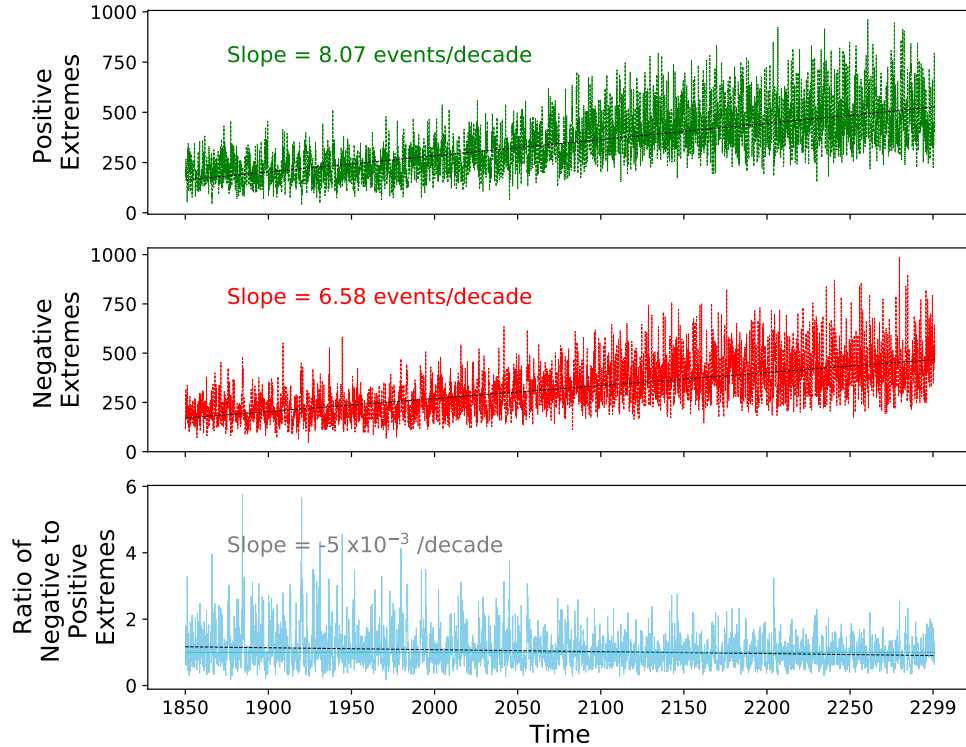


Figure 3: Counts of extremes relative to the threshold of 1850–1999

3. The figure 4 shows that the associated carbon loss or loss in gross primary productivity (due to negative extreme events) is increasing at least 20 % faster than the carbon gain (due to positive extreme events). Therefore, the impact of negative extremes would be larger in the future and hence if other conditions remain the same, the uptake of the CO₂ by land sink would reduce significantly and the concentration of CO₂ would increase.

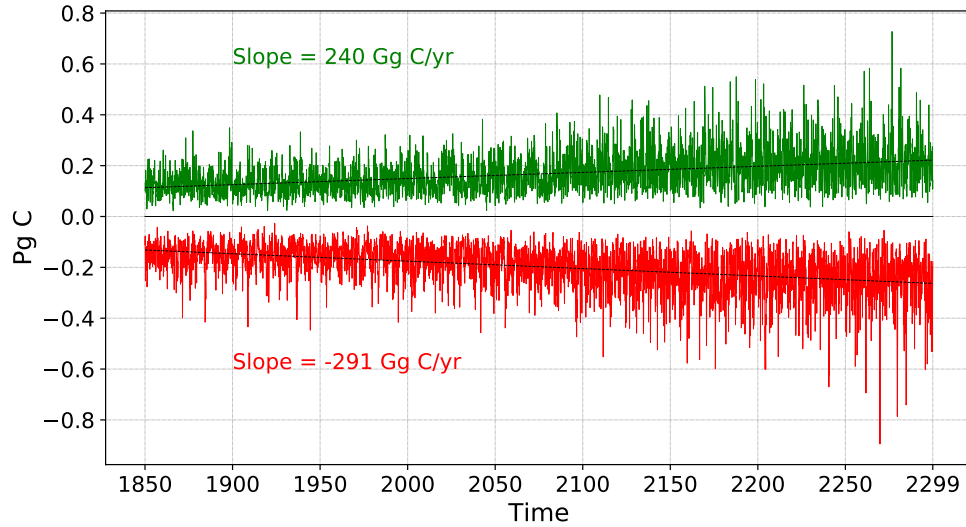


Figure 4: Global time-series of extreme events when percentile is 1.0 and time period is 25 years

4. The figure 5 shows the absolute difference of negative GPP extremes from the reference time period of 1975–1999. The red color signifies the strengthening of the negative GPP extreme events while the green color signifies the weakening. Increasing red regions indicate that in the future, the spatial extent and the intensity of the negative extreme events would increase globally.
5. The figure 6 shows the difference of the total GPP from the reference time period of 1975–1999. The red color in this figure indicates the region where the gross primary productivity is decreasing with time, while the green color is associated the increase in the gross primary productivity. There is an increase in the GPP due to the positive feedback, increased CO₂ and increased precipitation.
6. The reasons for the weakening of the negative GPP extreme events (see figure 5) was investigated at following regions (see figure 7):
 - (A) In and around Amazon basin

- (B) North of the South American tropics
- (C) Central South American tropics
- (D) South of the South American tropics

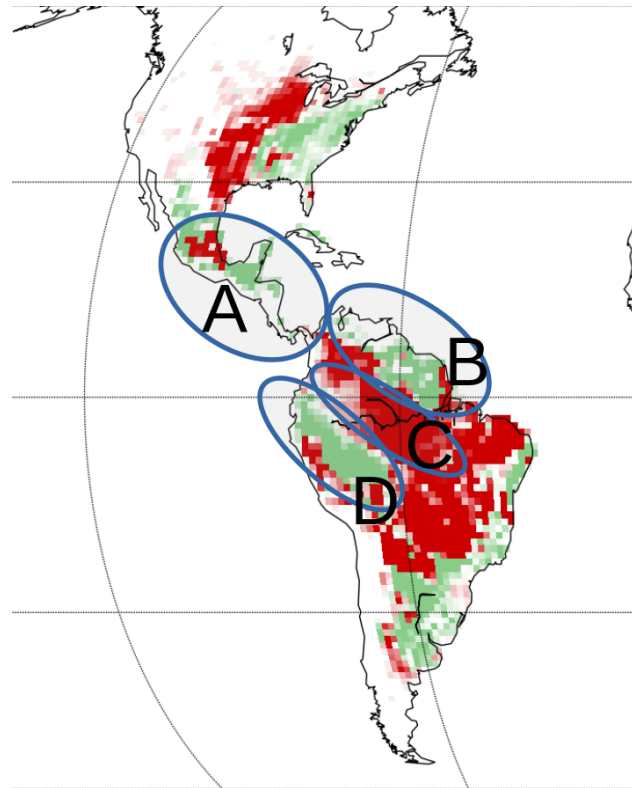


Figure 7: Changing patterns of the negative GPP extremes in and around South American tropics

Firstly, in the regions **A** and **B** we can see a decrease in the primary productivity (refer fig 6) after 2100 mainly due to the circulation changes, increase in the temperature and decrease in the precipitation. This leads to the mortality of the vegetation in these regions. Hence, the reduction in the GPP leads to reduced anomalies and extreme events. Therefore, weakening of the negative extreme events (refer fig 5) in the regions **A** and **B** is mainly due to vegetation dieback. Secondly, in the region **C**, the strengthening of the negative extremes (refer fig 5) is compensated by the increase in the primary productivity (refer fig 6). Lastly, due to the increasing positive feedback, and increase in the precipitation and nitrogen mineralization there is an increase in the primary productivity (refer fig 6) and spatial cover in the region **D**. Therefore, we see the weakening of the negative extreme events (refer fig 5) in this region.

7. The correlation of the anomalies of most climate drivers (Precipitation, Soil Moisture, Monthly Maximum Temperature and Precipitation–Evapotranspiration) was highest with the GPP anomalies and extremes when there was no time lag.
8. Using Multi Linear Regression, the case where there is no time lag and all climate drivers are considered, has the maximum adjusted R-squared values and indicated the best linear relationship (see table 1).

Table 1: Different Cases using Multi Linear Regression; numbers = prior month lag; **X** = excluded

Cases	Prcp	Soilmoist	T _{max}	P-ET	Fire	Rsq.adj
Case 1	0	0	0	0	0	0.5813
Case 2	1	1	1	1	1	0.4094
Case 3	2	2	2	2	2	0.3369
Case 4	0	0	0	0	1	0.5531
Case 5	0	0	0	1	0	0.4033
Case 6	0	0	1	0	0	0.5651
Case 7	0	1	0	0	0	0.5768
Case 8	1	0	0	0	0	0.4361
Case 9	0	0	0	0	X	0.5361
Case 10	0	0	0	X	0	0.4022
Case 11	0	0	X	0	0	0.5503
Case 12	0	X	0	0	0	0.5545
Case 13	X	0	0	0	0	0.4209
Case 14	0	X	X	X	X	0.3394
Case 15	X	X	X	0	X	0.3195
Case 16	0	X	X	0	X	0.4672

9. The dominant climate driver which has the strongest linear relationship with the carbon cycle extreme events for the case 1 (see table 1) was Precipitation–Evapotranspiration, followed by the Precipitation (see figure 8).

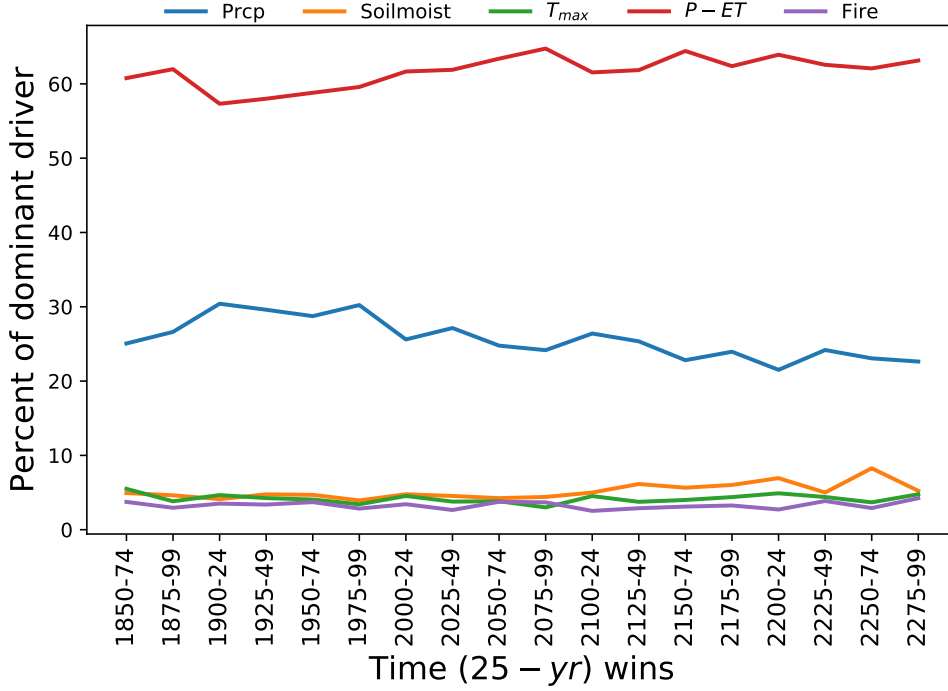


Figure 8: Dominant Climate Driver Time-series

3 Additional Participation

A part of this project titled “Carbon Cycle Extremes in the 22nd and 23rd Century and Attribution to Climate Drivers” was presented at the American Geophysical Union (AGU) Fall Meeting at New Orleans on Dec 15, 2017 in the session “Integrated Understanding of Climate, Carbon, Nutrient Cycles, Human Activities, and Their Interactions in Terrestrial Ecosystems II.” The talk was well-received and I received positive feedback from many people.

4 Overall Experience

The project I worked on, the people I worked with and the resources I had, all contributed towards the successful completion of the project. I have talked to almost every person in the CCSI and discussed some part of my project. Everyone has been very helpful and supportive. My advisers, Dr. Forrest M. Hoffman

and Dr. Jitendra Kumar have been very patient and great teachers throughout the project. They both have great work-life balance and have encouraged me to maintain it. All the administrative staff has been proactive in helping us with all the formalities, paperwork and paycheck processing. This experience has not only enhanced my professional network but also my personal network, both within and outside the lab. It was a great journey and I would be fortunate to work here again.

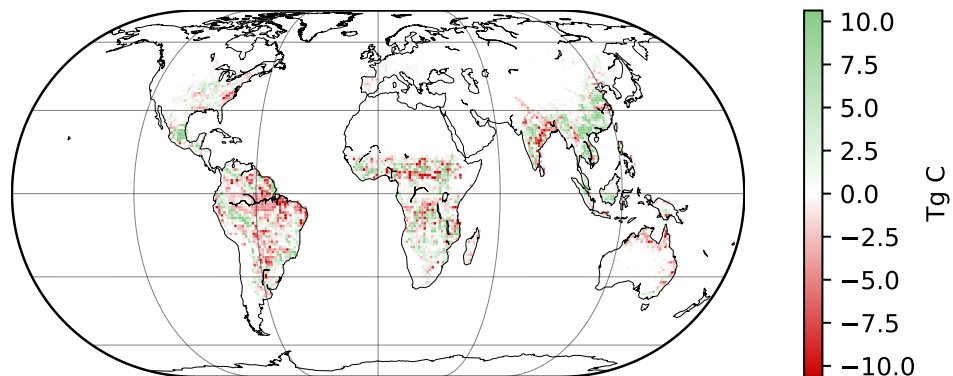
Open Research

Data Availability Statement

The CESM1(BGC) model output Sharma and Hoffman (2022) used for detection and attribution of carbon cycle extremes in the study are available at doi:10.5281/zenodo.5548153. Data analysis was performed in Python, and all analysis codes are publicly available on GitHub (Sharma, 2022b) at github.com/sharma-bharat/Codes_Carbon_Extremes_2300 and archived at doi:10.5281/zenodo.6147120.

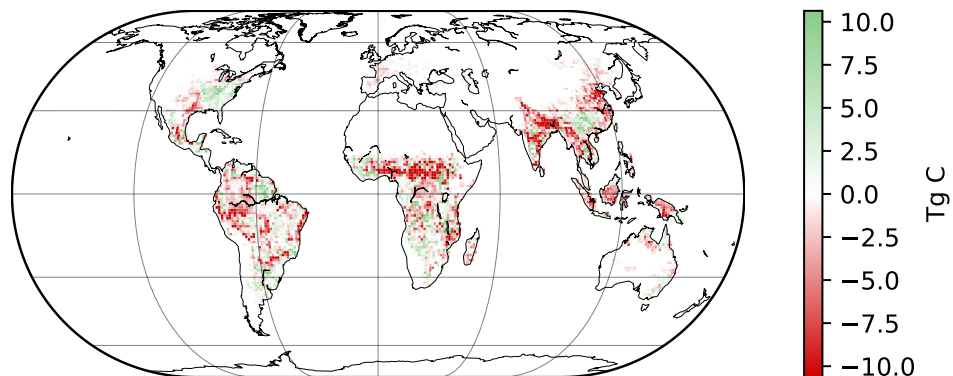
This collaboration with ORNL led to several papers Warner et al. (2019); Sharma et al. (2023, 2022b,a); Sharma (2022a); Massoud et al. (2024).

Absolute difference of negative gpp extremes
1925-49 - 1975-99



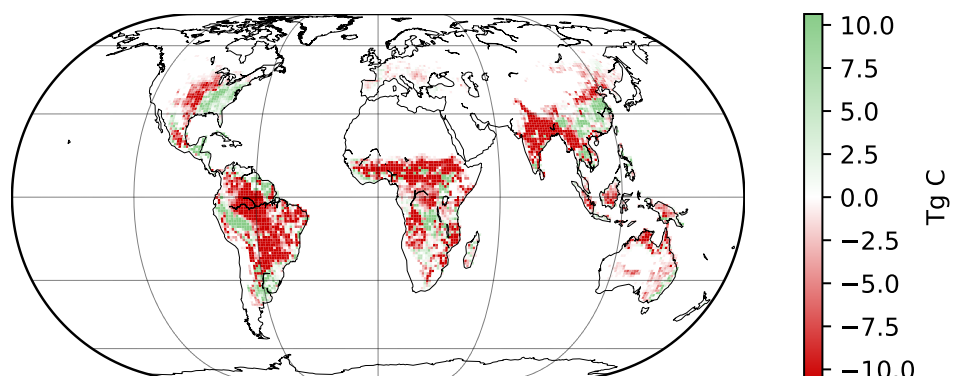
(a)

Absolute difference of negative gpp extremes
2025-49 - 1975-99



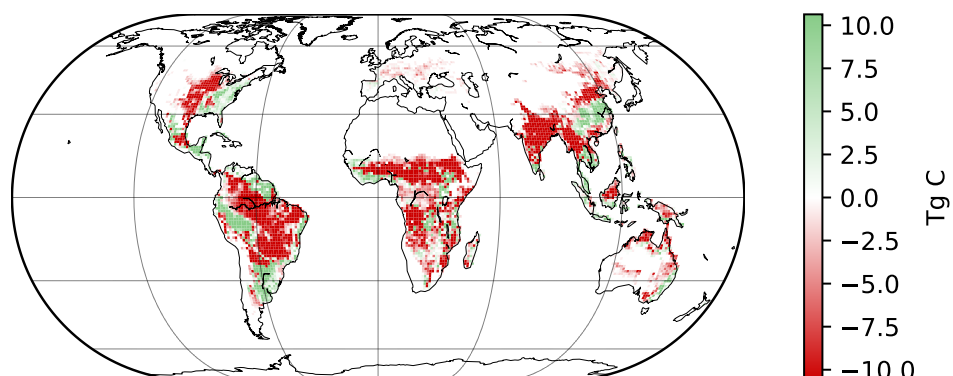
(b)

Absolute difference of negative gpp extremes
2125-49 - 1975-99



(c)

Absolute difference of negative gpp extremes
2225-49 - 1975-99



(d)

Figure 5: The difference of the negative GPP extremes compared to the 1975–1999

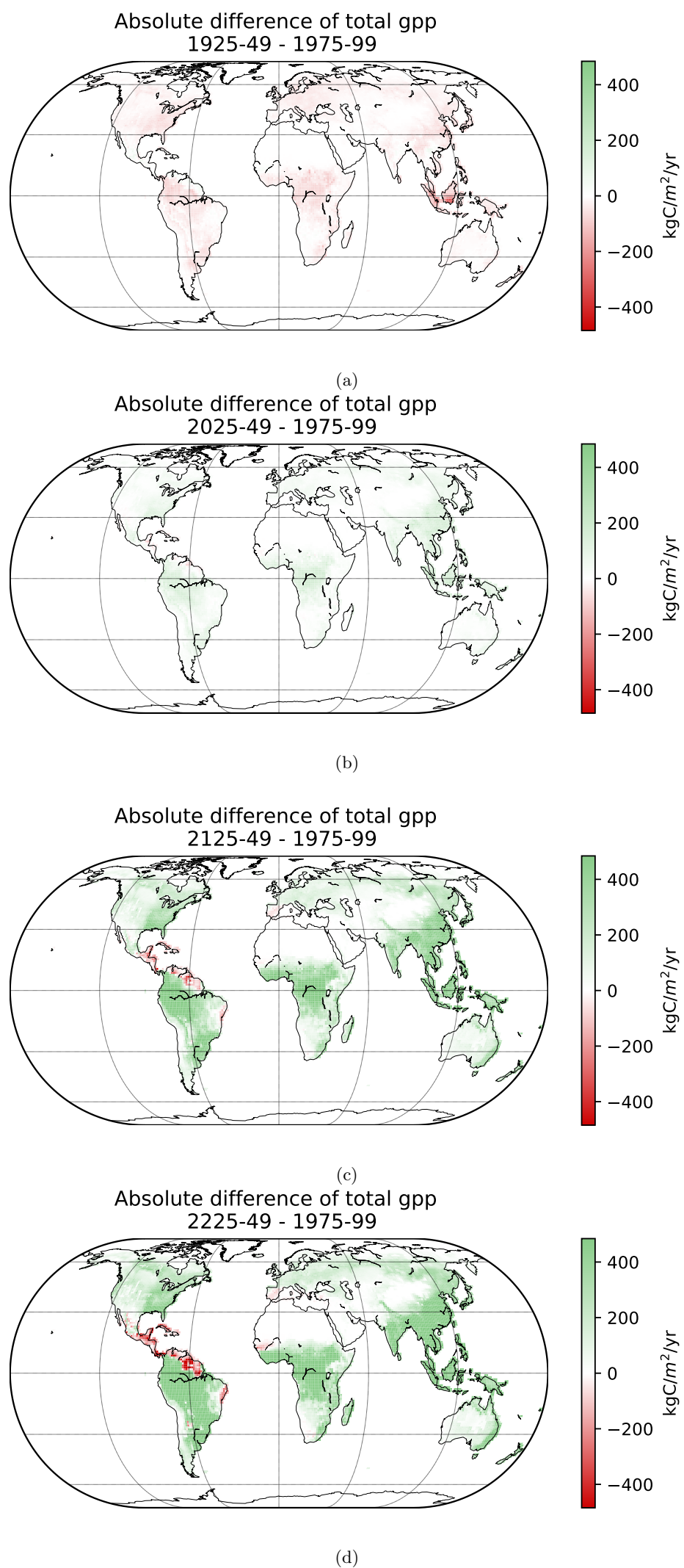


Figure 6: The difference of the total GPP compared to the 1975–1999

References

- Massoud, E. C., Collier, N., Sharma, B., Kumar, J., and Hoffman, F. M. (2024). Enhancing photosynthesis simulation performance in esms with machine learning-assisted solvers. In *2024 IEEE International Conference on Big Data (BigData)*, pages 4351–4356.
- Sharma, B. (2022a). *Analysis of Global Carbon Cycle Extremes, Their Compound Climate Drivers, and Implications for Terrestrial Carbon Cycle*. PhD thesis, Northeastern University.
- Sharma, B. (2022b). sharma-bharat/codes_carbon_extremes_2300: Analysis of carbon cycle extremes using earth system models. <https://doi.org/10.5281/zenodo.6147120>. Zenodo code repository available at <https://zenodo.org/record/6147120>.
- Sharma, B. and Hoffman, F. M. (2022). Selected land variables from cesm1(bgc) simulations for 1850 to 2300. <https://doi.org/10.5281/zenodo.5548153>. Zenodo dataset available at <https://zenodo.org/record/5548153>.
- Sharma, B., Kumar, J., Collier, N., Ganguly, A. R., and Hoffman, F. M. (2022a). Quantifying carbon cycle extremes and attributing their causes under climate and land use and land cover change from 1850 to 2300. *Journal of Geophysical Research: Biogeosciences*, 127(6):e2021JG006738. e2021JG006738 2021JG006738.
- Sharma, B., Kumar, J., Ganguly, A. R., and Hoffman, F. M. (2022b). Using image processing techniques to identify and quantify spatiotemporal carbon cycle extremes. In *2022 IEEE International Conference on Data Mining Workshops (ICDMW)*, pages 1136–1143.
- Sharma, B., Kumar, J., Ganguly, A. R., and Hoffman, F. M. (2023). Carbon cycle extremes accelerate weakening of the land carbon sink in the late 21st century. *Biogeosciences*, 20(10):1829–1841.
- Warner, M., Sharma, B., Bhatia, U., and Ganguly, A. (2019). Evaluation of Cascading Infrastructure Failures and Optimal Recovery from a Network Science Perspective. In Ghanbarnejad, F., Saha Roy, R., Karimi, F., Delvenne, J.-C., and Mitra, B., editors, *Dynamics On and Of Complex Networks III*, pages 63–79, Cham. Springer International Publishing.